COPY 2

UCRL-1465

UNCLASSIFIED

UNIVERSITY OF CALIFORNIA — BERKELEY

TWO-WEEK LOAN COPY

This is a Library Circulating Copy which may be borrowed for two weeks. For a personal retention copy, call Tech. Info. Division, Ext. 5545

RADIATION LABORATORY

DISCLAIMER

This document was prepared as an account of work sponsored by the United States Government. While this document is believed to contain correct information, neither the United States Government nor any agency thereof, nor the Regents of the University of California, nor any of their employees, makes any warranty, express or implied, or assumes any legal responsibility for the accuracy, completeness, or usefulness of any information, apparatus, product, or process disclosed, or represents that its use would not infringe privately owned rights. Reference herein to any specific commercial product, process, or service by its trade name, trademark, manufacturer, or otherwise, does not necessarily constitute or imply its endorsement, recommendation, or favoring by the United States Government or any agency thereof, or the Regents of the University of California. The views and opinions of authors expressed herein do not necessarily state or reflect those of the United States Government or any agency thereof or the Regents of the University of California.

UCRL 1465
SEP 6 1951

NUCLEAR EXCITATION AND RECOIL BY HIGH ENERGY PARTICLES

By

Si-Chang Fung
B.S. (Chiao-Tung University) 1939
M.S. (State College of Washington) 1949

DISSERTATION

Submitted in partial satisfaction of the requirements for the degree of

DOCTOR OF PHILOSOPHY

in

Chemistry

in the

GRADUATE DIVISION

of the

UNIVERSITY OF CALIFORNIA

Approved:

.....

.....

.....
Committee in Charge

Deposited in the University Library.....
Date Librarian

NUCLEAR EXCITATION AND RECOIL BY HIGH ENERGY PARTICLES

Si-Chang Fung
Radiation Laboratory and Department of Chemistry
University of California, Berkeley, California

ABSTRACT

Part I. The less probable nucleon-capture reaction induced by high energy particles has been investigated in order to see what is the highest possible energy of a nucleon to be able to stay inside the nucleus. Excitation curves of $Bi^{209}(d,p)Bi^{210}$, $Bi^{209}(d,n)Po^{210}$, $Bi^{209}(d,3n)Po^{208}$, $Bi^{209}(d,5n)Po^{206}$, $Bi^{209}(\alpha,2pn)Bi^{210}$, $Bi^{209}(\alpha,p4n)Po^{208}$, and $Bi^{209}(\alpha,p6n)Po^{206}$ have been determined. The cross section of $Al^{27}(\alpha,\alpha 2pn)Na^{24}$ reaction with 340 Mev alpha particles has also been determined. The experimental data indicate that the (d,p) and (d,n) reactions on bismuth are mainly due to the capture of a neutron or a proton in zero or negative energy state or with a positive energy up to several Mev during stripping. The experimentally observed cross sections decrease with energy above 100 Mev much more rapidly than the Peaslee's expression indicates. It seems probable that the sticking probabilities ξ_p and ξ_n are decreasing functions of the energy in the high energy region. The (α,2pn) reaction are likely to be due to the formation of compound nucleus followed by evaporation of one neutron and two protons, although it can equally adequately be considered to proceed by the absorption of a neutron in zero or negative energy state or with a positive energy up to several Mev due to the relative motion of neutrons inside the helium ion with respect to the center of mass of that helium ion.

Part II. The energy dependence of the forward recoil loss of Na^{24} produced in aluminum foil by bombardment with high energy protons, deuterons, and helium ions has been thoroughly investigated. In low energy regions, the recoil loss which checks reasonably well with the calculated values (with the assumption compound nucleus model) increases as the energy of incident particle increases, which is consistent with compound nucleus formation as postulated by Bohr. The percentage of recoil then passes through a maximum and decreases as the energy of incident particle increases. Therefore it clearly shows that the high energy incident particle transfers only part of its energy to the target nucleus by making one or more collisions with nucleon or nucleons inside as it passes through in these particular nuclear reactions.

Table of Contents (Part I)

		Page
I.	INTRODUCTION	7
II.	EXPERIMENTAL	9
	A. Preliminary work	9
	B. Preparation of target	10
	C. Bombarument and Determination of Beam Intensity	11
	D. Procedure for the Isolation of Polonium from Bismuth	12
	E. Determination of Absolute Cross Section of $Al^{27}(\alpha,\alpha 2pn)Na^{24}$ Reaction with 340 Mev Alpha Particles	15
III.	EVALUATION OF DATA AND RESULTS	17
IV.	DISCUSSION AND CONCLUSION	24
	FIGURES	29
	REFERENCES	38

List of Figures (Part I)

Figure 1. Excitation curves of (d,p), (d,n), (d,3n), and (d,5n) reactions on bismuth.

Figure 2. Excitation curves of (α,2pn), (α,p4n), and (α,p6n) reactions on bismuth.

Figure 3. Alpha pulse analysis of a standard sample of Po^{208} - Po^{209} - Po^{210}.

Figure 4. Alpha pulse analysis of a sample of polonium isotopes produced during the bombardment of bismuth with 140 Mev deuteron together with a small amount of Po^{210} grown in from Bi^{210}, measured at the same time as the standard in Figure 3.

Figure 5. Alpha pulse analysis of a sample of Po^{210} which grew in from the beta minus decay of Bi^{210} produced in the same bombardment as in Figure 4, measured at the same time as the standard in Figure 3.

Figure 6. Excitation Curve of $Al^{27}(p,3pn)Na^{24}$ reaction by P. C. Stevenson and R. L. Folger.

Figure 7. Excitation curve of $Al^{27}(d,p\alpha)Na^{24}$ reaction by W. W. Meinke.

Figure 8. Excitation curve of $Al^{27}(\alpha,\alpha 2pn)Na^{24}$ reaction by A. C. Helmholz.

Figure 9. A graph plotting the log of cross section against the log of deuteron energy for (d,p) and (d,n) reactions on bismuth. The attenuation of the beam was corrected by the following formula:

$$I = I_o e^{-\sigma x n} \text{ , with } \sigma = \frac{\pi}{2} \quad R_d R + 2 \pi R^2$$

where x = thickness of copper plate the beam passed in order to decrease the incident energy of deuterons to the desired energy.

n = number of copper atoms per cubic centimeter.

I_o = initial beam intensity.

I = beam intensity after passing through x cm of copper.

σ = total cross section for stopping the beam.

R_d = radius of deuteron defined by Serber.[9]

R = radius of copper nucleus.

NUCLEAR EXCITATION AND RECOIL BY HIGH ENERGY PARTICLES

Si-Chang Fung
Radiation Laboratory and Department of Chemistry
University of California, Berkeley, California

NUCLEAR EXCITATION OF BISMUTH WITH HIGH ENERGY PARTICLES

I. INTRODUCTION

Spallation and fission have long been considered in this laboratory to be the two interesting aspects of nuclear reactions induced by the high energy nuclear particles. It is of interest to us to investigate the less probable nucleon-capture reactions which may throw some light upon the question of how much energy a nucleus can dissipate without losing nucleons. Bismuth is our favored choice as target for the investigation of (d,p), (d,n) and (α,2pn) reactions for the following reasons.

(1) Single isotope of mass number 209.

(2) Po^{210} formed by capture of a proton is an alpha emitter. A carrier free sample can be prepared and its activity can be fairly accurately determined.

(3) Bi^{210} formed by neutron capture decays by β^- emission into Po^{210} with a half-life of 5.0 days. The polonium fractions, produced during the bombardment, was separated completely from bismuth right after the irradiation. From the Po^{210} grown in, we can calculate the cross section of the $Bi^{209}(d,p)Bi^{210}$ reaction.

Kelly and Segrè[1] have determined the (d,p), (d,n), (α,2n), and (α,3n) reactions on bismuth with deuteron energy up to 18.7 Mev and alpha energy up to 38.8 Mev. The (α,2n) and (α,3n) reactions were explained as compound nucleus formation and subsequent evaporation of two or three neutrons.

The (d,p), and (d,n) reactions, were considered to be mainly due to the stripping processes which were treated theoretically by Peaslee.[2]

Peaslee considers that practically the entire (d,p) cross section at any bombarding energy of deuteron (E_d) arise from a stripping process in which the neutron is captured by the nucleus, while the proton misses and continues on its way, and the (d,n) excitation curve is also predominantly due to the stripping process with proton and neutron inside the deuteron interchanging their feature for $E_d \gtrsim 10$ Mev. Furthermore it is assumed that the stripping process can only take place if the escaping nucleon carries away all the incident energy or even more, leaving the captured neutron or proton in a negative energy (bound) state in the final nucleus, which can be visualized as occurring by a favorable partitioning of internal energy of the deuteron governed by its internal wave function. As the energy of the nucleon is measured from a zero corresponding to the potential energy of infinite separation from the nucleus, a nucleon bound in the nucleus is defined as a "negative energy" nucleon. Finally, he predicted that the ratio of (d,p) and (d,n) cross sections may approach the limit of $\xi_n/\xi_p \approx 1$ as E_d increases indefinitely, where ξ_n and ξ_p are the average "sticking probabilities" of neutrons and protons.

The purpose of this study is to investigate the excitation functions of the (d,n), (d,p), and (α,2pn) reactions with deuteron and helium ion energy above 40 Mev to see what is the highest possible energy of a nucleon to be able to stay inside the nucleus.

II. EXPERIMENTAL

A. Preliminary Work

In order to determine the yield of polonium quantitatively, we have tried to separate a known amount of polonium activity from the bismuth solution. A carrier free polonium sample was diluted to 5 ml with 6 N HCl in a volumetric flask. Ten λ of it was mounted on a platinum counting disk as sample A. The remaining solution was transferred to a 15 ml centrifuge tube. After the addition of 20 mg of bismuth, the solution was evaporated to almost dryness on a water bath under a gentle air jet across the top of the tube. The residue was dissolved in 1 ml of concentrated HCl and the resulting solution was again evaporated almost to dryness. The last step was repeated three times to decompose all nitrate ion present in the solution. The residue was then dissolved in 1.5 ml of 6 N HCl and the resulting solution was extracted twice with 1.5 ml of 80 percent dibutyl ether, 20 percent tributyl phosphate by volume mixture (TBP). The TBP extracts which contained almost all the polonium was washed twice with 1 ml 6 N HCl to remove bismuth completely. The polonium was then re-extracted into an aqueous layer when the TBP layer was contacted twice with 1.5 ml 4 N HNO_3, 2 N HCl mixed acids solution. The nitrate ion in aqueous layer was decomposed by successive additions of concentrated HCl and evaporation as before. The residue was dissolved in 6 N HCl and the resulting solution was completely transferred to original 5 ml volumetric flask. Additional 6 N HCl was added to fill the flask to the mark. Ten microliters of it was mounted on the platinum counting disk as sample B. The remaining

solution was treated with exactly the same procedure as that after the preparation of sample A. The sample C was then prepared. The polonium activities of these three samples were counted on the same alpha counter. The average counts per minute were as follows:

Sample A	4510 ± 20
Sample B	4620 ± 30
Sample C	4465 ± 35

Moreover, only negligible alpha activities were found in bismuth fractions, HCl washings and the remaining TBP fractions. Therefore we can safely consider that the yield of polonium was very close to one hundred percent.

B. Preparation of Target

Approximately 200 mg of pure bismuth metal was melted on an aluminum foil of 1 inch x 1 inch in size and 0.001 inch thick. The bismuth was evenly distributed on an area of approximately 3 square centimeters. This bismuth-aluminum foil together with a same size 0.5 mil aluminum foil which was used as monitor to determine the beam intensity inside the Berkeley 184-inch cyclotron, were mounted in a clamp type target holder in the order of bismuth layer, 1 mil aluminum foil and 0.5 mil aluminum foil as was seen by the beam. The edges of the rectangular shaped foils were cut flush with one another, so that the beam will hit the bismuth layer and monitor in exactly the same areas.

C. Bombardment and Determination of Beam Intensity

After the bombardment (approximately 45 minutes), the foils were cut into equal and corresponding areas. Approximately 24 hours later, the 0.5 mil aluminum foil (monitor) was weighed and mounted on a scotch-tape counting plate and counted every four to eight hours for 60 hours on the second shelf of a Geiger-Müller counter. The activity in counts per minute was plotted against time on a three-cycle semi-log paper. The activity of Na^{24} in aluminum foil produced during bombardment was determined by drawing a 15 hour half-life line through these points and extrapolating to the mid-point of the bombardment. The counting efficiency and geometrical correction was determined by measuring both alpha and beta minus activities of an equilibrium mixture of RaD, E, and F, mounted on a platinum plate. The counting yield for alpha particles in the 2π geometry chamber is considered to be 52 percent. The β^- activity was counted on the second shelf of a Geiger-Müller counter. The correction to zero-back-scattering was made by dividing the counts per minute with the total back-scattering of lead by 1.80. By the above comparison, the counting efficiency of β^- activity of the sample with zero back-scattering on the second shelf of the Geiger-Müller counter was 2.54 percent. The counting efficiency was again checked to be 2.49 percent by using McMillan's beta standard (U_2O_6) which was taken as standard in determining the excitation function of ${}_{13}Al^{27}(d,d2pn){}_{11}Na^{24}$ reaction. The counting efficiency of 2.50 percent together with the known cross section of $Al^{27}(d,p\alpha)Na^{24}$, and $Al^{27}(\alpha,\alpha 2pn)Na^{24}$ reaction at various energies[3] (see Figures 7 and 8). The cross section of

$Al^{27}(d,p\alpha)Na^{24}$ reaction is 48 millibarns with 194 Mev deuterons.) was used to determine the average intensity of the deuteron or alpha beam during the bombardment.

The thin target formula was used for calculation:

$$N = IN_0 (\Delta X)\sigma t$$

$$\Delta X = W/dA$$

$$P = It/A = Nd/WN_0\sigma \qquad (1)$$

where N = number of Na^{24} atoms formed

N_0 = number of atoms of Al^{27} per cubic centimeter

ΔX = thickness of the aluminum foil

σ = cross section

I = beam intensity

t = time of bombardment

W = weight of the foil

d = density of aluminum

A = area of the target

Since A, t, and I are the same for bismuth and aluminum, this factor P was later used directly for the calculation of cross sections of any nuclear reaction on bismuth.

D. Procedure for the Isolation of Polonium from Bismuth

The bismuth-aluminum foil was dissolved right after the cutting in 4 ml of aqua regia in a 40 ml centrifuge tube. The nitrate ion was completely destroyed by successive evaporation with concentrated HCl as in the preliminary work. The final chloride residue was dissolved

in 5 ml 6 N HCl. The resulting solution was extracted seven times with 3 ml portions of TBP. The first four extracts were mixed together as fraction A, the following two extracts as fraction B and the last extract as fraction C. The time for the final extraction was recorded as t_1. Two portions of 5 ml 6 N HCl were used in washing three fractions of TBP extracts in the order of A, B, C. The washings which remove all the bismuth but no polonium from the TBP extracts were added to the original bismuth fraction. The TBP fractions were then extracted in the order of C, B, A with four portions of 5 ml 4 N HNO_3 - 2 N HCl solution which remove quantitatively the polonium from TBP layers. The aqueous polonium layer was evaporated almost to dryness and converted completely to chlorides by successive evaporation with concentrated HCl as before. The residue was then dissolved in 6 N HCl and the resulting solution was completely transferred to 5 ml volumetric flask. Additional 6 N HCl was added to fill the flask to the mark. Two hundred to six hundred microliters were mounted on a platinum counting disk and the decay of the carrier free polonium (I) sample was followed. This polonium sample contained mainly 9 day Po^{206}, 2.93 year Po^{208}, and 138 day Po^{210} which were produced during the bombardment with some Po^{210} which grew in from Bi^{210} within a time interval ($t_1 - t_o$) where t_o is the time of the middle of the bombardment. Approximately two months later, a polonium sample chemically plated on silver foil from 2 N HCl solution was alpha pulse analyzed.[4] From the graph of plotting activity against energy of emitted alpha particles (see Figure 4), we can calculate the ratios of activities between various polonium isotopes.

Approximately seven days after the bombardment, the Po^{210} which grew in from Bi^{210} in bismuth fraction was extracted and treated exactly the same as described before. The time of last extraction was recorded as t_2. Three twenty-fifths to one-half of the polonium activity was mounted on a platinum disk (Sample II). The decay of the sample (II) has always shown a half-life of 138 days. The alpha pulse analysis activity which grew from the bismuth showed a single peak corresponding to Po^{210}. This indicated that the Po^{210} in sample (II) was exclusively derived from the decay of Bi^{210}. After another 20 days, the Po^{210} which grew was again extracted and treated as before. The time for the last extraction was recorded as t_3. Likewise, sample (III) was prepared and decayed with a half-life of 138 days. The alpha pulse analysis of the chemically plated sample showed again a single peak corresponding to Po^{210}. (See Figure 5.)

Bismuth in the aqueous layer was then precipitated as bismuth sulfide by passing H_2S into a solution of 0.3 N hydrogen ion concentration while aluminum remained in the solution. After being washed twice with 5 ml portion of saturated H_2S water of pH value 1, the bismuth sulfide was dissolved in concentrated HCl. Following the complete expelling of H_2S by boiling, the bismuth was determined as BiOCl. Three experiments of determining known amount of bismuth as BiOCl have been carried out with an error of less than 0.7 percent.

The formation of Bi^{210} from Bi^{209} by neutron capture process from stray neutrons was checked by bombarding bismuth with high energy protons using the assumption that the neutron flux from this source would be of

the same order as that from high energy deuterons or alpha particles. The target preparation and procedure of experimentwere exactly the same as the case of deuteron and alpha particle bombardment. The cross sections of forming Bi^{210} with several different energy of protons were determined. The beam intensity of protons was determined from the known excitation function of $Al^{27}(p,3pn)Na^{24}$ reaction.[5] (See Figure 6.)

E. Determination of Absolute Cross Section of $Al^{27}(\alpha,\alpha 2pn)Na^{24}$ Reaction with 340 Mev Alpha Particles

This cross section was determined by using graphite as monitor. The cross section of $C^{12}(\alpha,\alpha n)C^{11}$ reaction with 340 Mev alpha particles was determined to be 60.5 ± 0.6 millibarns.[6] The procedure of experiment was as follows: Two sheets of 10 mil graphite and four layers of 0.5 mil aluminum foils were arranged in above order as was seen by the beam and mounted in a clamp type target holder. The edges of the rectangular shaped foils were flush with one another. After the bombardment (3 - 10 minutes) the foils were immediately cut into equal and corresponding areas. The two graphite layers were weighed and mounted separately on the same type scotch-tape counting plates and counted every five to ten minutes for approximately 270 minutes, first on the fifth shelf with beryllium absorber of 704 mg/cm^2 on second shelf, then on fifth shelf without beryllium absorber and finally on the second shelf of the same Geiger-Müller counter. The ratio of three different cases of counting was carefully determined. The activity in counts per minute converted to second shelf was then plotted against time on a four-cycle

semi-log paper. The activity of C^{11} produced during bombardment can be obtained by following formula:

$$T = Rt = Gtk^{-1} (1 - e^{-\lambda_5 t})^{-1}$$

where R = number of atoms of C^{11} produced in unit time interval

t = time of bombardment

G = activity of C^{11} in counts per unit time extrapolated to the end of bombardment

k = counting efficiency

λ_5 = decay constant of C^{11}

By use of thin target formula, the average beam intensity can be evaluated:

$$I = RA/n\sigma$$

where A = area of the target

n = total number of carbon atoms in the target

σ = cross section of formation of C^{11} from graphite with 340 Mev alpha particles.

Approximately 24 hours later, the aluminum foils were weighed and mounted separately on the scotch-tape counting plate and counted every four to eight hours on the second shelf of the same Geiger-Müller counter for 60 hours. The average activity of Na^{24} in the second, third, and fourth foils which contained almost the same amount of Na^{24} activity was extrapolated to the middle of the bombardment.

The cross section of $Al^{27}(\alpha,\alpha 2pn)Na^{24}$ reaction can be evaluated as follows:

$$\sigma = HA/k\lambda In_o t$$

where H = activity in counts per minute of Na^{24} in aluminum foil extrapolated to the middle of the bombardment

k = counting efficiency

λ = decay constant of Na^{24}

n_o = total number of aluminum atoms in aluminum foil (using average weight of three foils which had a difference in weight within one percent).

III. EVALUATION OF EXPERIMENTAL DATA AND RESULTS

From the experimental data, we can calculate the cross sections of $Bi^{209}(d,p)Bi^{210}$, $Bi^{209}(\alpha,\alpha 2pn)Bi^{210}$, $Bi^{209}(d,n)Po^{210}$ and some other reactions. The number of atoms of Bi^{210} formed during the bombardment can be determined from either the Po^{210} activity of sample (II) or that of sample (III). The reasonable check of those two values will show the accuracy of the experiments and give an additional proof of the origin of Po^{210} from the decay of Bi^{210} which was formed during the bombardment.

The formulas for calculating the number of atoms of Bi^{210} are as follows:

$$N_1^o(II) = \frac{A_2}{(0.52)X_2} \cdot \frac{(\lambda_2 - \lambda_1)}{\lambda_1\lambda_2} e^{\lambda_1(t_1-t_o)} \left[e^{-\lambda_1(t_2-t_1)} - e^{-\lambda_2(t_2-t_1)}\right]^{-1}$$

$$N_1^o(III) = \frac{A_3}{(0.52)X_3} \cdot \frac{(\lambda_2 - \lambda_1)}{\lambda_1\lambda_2} e^{\lambda_1(t_2-t_o)} \left[e^{-\lambda_1(t_3-t_2)} - e^{-\lambda_2(t_3-t_2)}\right]^{-1}$$

where $N_1^o(II)$ = number of atoms of Bi^{210} calculated from sample (II)

$N_1^o(III)$ = number of atoms of Bi^{210} calculated from sample (III)

A_2 = Po^{210} activity (C/m) of sample (II) extrapolated to t_2

A_3 = Po^{210} activity of sample (III) extrapolated to t_3

X_2 = fraction of activity of the second series of extractions mounted as sample (II)

X_3 = fraction of activity of the third series of extractions mounted as sample (III)

λ_1 = decay constant of Bi^{210}

λ_2 = decay constant of Po^{210}

The number of atoms of each isotope of polonium (Po^{210}, Po^{208}, Po^{206}) can be evaluated from the pulse analysis data of the polonium activity of the first series of extractions and the activity of sample (I).

The graph of plotting activity against energy from the alpha pulse analysis data showed two or three peaks of alpha energies corresponding to Po^{210}, Po^{208} or Po^{210}, Po^{208} and Po^{206} with negligible amounts of unknown activities. At time t (time for alpha pulse analysis) if the activity under each peak were a(Po^{210}), b(Po^{208}), c(Po^{206}), and activity of sample (I) were g, the activity of Po^{210}, Po^{208}, Po^{206} in sample (I) theoretically extrapolated to t_o would be

$$A_1 = \frac{ag}{a + b + c} e^{\lambda_2(t - t_o)} \qquad (Po^{210})$$

$$B_1 = \frac{bg}{a + b + c} e^{\lambda_3(t - t_o)} \qquad (Po^{208})$$

$$C_1 = \frac{cg}{a + b + c} e^{\lambda_4(t - t_o)} \qquad (Po^{206})$$

where λ_3 = decay constant of Po^{208}

λ_4 = decay constant of Po^{206}

C_1 can also be determined from the decay curve of sample (I).

Then the number of atoms of Po^{210}, Po^{208}, and Po^{206} formed during the bombardment can be evaluated:

$$M = \frac{A_1}{(0.52)X_1\lambda_2} - \frac{N_1^{o}(II) + N_1^{o}(III)}{2}\left[1 - e^{-\lambda_1(t_1-t_o)}\right]$$

$$L = \frac{B_1}{(0.52)X_1\lambda_3}$$

$$K = \frac{C_1}{(0.52)X_1\lambda_4 q}$$

where M = number of atoms of Po^{210} formed during bombardment

L = number of atoms of Po^{208} formed during bombardment

K = number of atoms of Po^{206} formed during bombardment

X_1 = fraction of activity of first series of extractions mounted as sample (I)

q = fraction of decay of Po^{206} by alpha emission.

The cross sections can easily be shown to be

$$\sigma_1(II) = N_1^{o}(II)\,\frac{d'}{PW'n}$$

$$\sigma_1(III) = N_1^{o}(III)\,\frac{d'}{PW'n}$$

$$\sigma_2 = \frac{Md'}{PW'n}$$

$$\sigma_3 = L \cdot \frac{d'}{PW'n}$$

$$\sigma_4 = K \cdot \frac{d'}{PW'n}$$

where $\sigma_1(II)$ = cross section of $Bi^{209}(d,p)Bi^{210}$ or $Bi^{209}(\alpha,2pn)Bi^{210}$ reaction calculated from sample (II)

$\sigma_1(III)$ = cross section of $Bi^{209}(d,p)Bi^{210}$ or $Bi^{209}(\alpha,2pn)Bi^{210}$ reaction calculated from sample (III)

σ_2 = cross section of $Bi^{209}(d,n)Po^{210}$ or sum of cross sections of $Bi^{209}(\alpha,3n)At^{210}$ and $Bi^{209}(\alpha,p2n)Po^{210}$

σ_3 = cross section of $Bi^{209}(d,3n)Po^{208}$ or $Bi^{209}(\alpha,p4n)Po^{208}$

σ_4 = cross section of $Bi^{209}(d,5n)Po^{206}$ or $Bi^{209}(\alpha,p6n)Po^{206}$

d' = density of bismuth

n = number of atoms per cubic centimeter of bismuth

The results will be summarized in Tables 1 - 4.

The discrepancy in the cross section of formation of Po^{206} by 220 Mev helium ions (experiment number 5) is most probably due to the contamination of the beam by deuterons.

Table I

The cross section of $Al^{27}(\alpha,\alpha 2pn)Na^{24}$ reaction with 340 Mev alpha particles

Experiment number	Cross section in millibarns
1	24.0
2	21.8
3	24.4
4	24.9
Average	23.8

Table II

The excitation functions of nuclear reactions on bismuth with high energy protons

Experiment number	Energy of particle in Mev	Cross section for formation of Bi^{210} based on proton beam but due to neutron background (in millibarns)	Cross section of formation of Po^{210} from Bi^{209} (p,γ reaction) (in millibarns)
1	100	0.007	$<10^{-3}$
2	120	0.007	$<10^{-3}$
3	180	0.011	$<10^{-3}$

Table III

The excitation functions of several nuclear reactions on Bismuth with high energy deuterons

Experiment number	Energy of particle (in Mev)	Cross section of formation on Bi^{210} (in millibarns) σ_1(II)	σ_1(III)	σ_1 average	Cross section of formation of Po^{210} (σ_2)	Cross section of formation of Po^{208} (σ_3)	Cross section of formation of Po^{206} times q*(σ_4 x q)
1	40	14.5	14.0	14.3	13.4 mb	315 mb	3.0 mb
2	40	13.8	13.9	13.9	13.9 mb	277 mb	11.3 mb
3	60	9.96	8.58	9.27	12.8 mb	258 mb	28.0 mb
4	80	4.47	4.50	4.49	11.0 mb	105 mb	17.1 mb
5	100	2.44	2.73	2.59	6.10 mb	63.2 mb	9.47 mb
6	120	1.56	1.56	1.56	4.57 mb	44.1 mb	6.68 mb
7	120	1.56	1.51	1.54	4.66 mb	50.6 mb	7.45 mb
8	140	0.921	0.901	0.911	2.66 mb	43.9 mb	5.16 mb
9	160	0.614	0.568	0.591	1.94 mb	28.8 mb	3.34 mb
10	180	0.283	0.335	0.309	1.15 mb	19.6 mb	2.40 mb
11	180	0.356	0.332	0.343	1.10 mb	22.1 mb	2.54 mb
12	190	0.340	0.420	0.380	1.33 mb	25.2 mb	3.00 mb

*q is the fraction of decay of Po^{206} by alpha emission.

Table IV

The excitation functions of several nuclear reactions on bismuth with high energy helium ions

Experiment number	Energy of particle (in Mev)	Cross Section of Formation of Bi^{210} (in millibarns) σ_1(II)	σ_1(III)	σ_1 average	Sum of cross sections of formation of Po^{210} and At^{210} (σ_2) in millibarns	Cross section of Formation of Po^{208} (σ_3) (in millibarns)	Cross section of formation of Po^{206} times q ($\sigma_4$xq) (in millibarns)
1	140	2.0_4	1.7_4	1.8_9	17.8	95.3	7.77
2	140	1.8_5	1.7_4	1.8_0	15.3	83.8	7.1_8
3	180	1.47	1.5_8	1.5_3	8.9_0	43.0	3.8_9
4	220	1.1_8	1.1_7	1.1_8	7.97	37.7	3.1_4
5	220	1.2_3	1.2_8	1.26	5.36	38.5	4.6_0
6	260	0.910	0.828	0.86_9	4.4_0	24.4	2.2_3
7	300	0.746	0.692	0.71_9	3.6_0	20.6	1.9_0
8	340	0.52_9	0.552	0.541	2.2_4	16.7	1.4_0
9	340	0.424	0.452	0.43_8	1.98	13.6	1.2_4

The cross sections in Tables III and IV have neither been corrected for the attenuation of beam nor the neutron background during the determination of excitation functions of formation of Na^{24} from Al^{27} by bombarding deuterons or alpha particles of various energies with the well-known stacked foil technique.

In our experiments, the neutron background causes negligible error in the determination of (d,p) and (α,2pn) reactions on bismuth as we can see that the cross sections of formation of Bi^{210} by bombarding bismuth with high energy protons are much smaller (see Table II) than that of (d,p) and (α,2pn) reactions.

IV. DISCUSSION AND CONCLUSION

In Figure 1 will be found plotted the data for the (d,p) and (d,n) reactions on bismuth with deuteron energy between 40 and 190 Mev. The excitation curve of Kelly and Segrè for deuteron energies 18 Mev and lower are also reproduced.

The most apparent difference between the (d,p) and (d,n) excitation functions is that the (d,p) cross sections are higher than (d,n) cross sections at the lower energies (up to and past the potential barrier energy) and that there is a reversal at high energies. The point of crossing is in the energy range not covered by the two sets of data and is probably between 30 and 40 Mev deuteron energy. According to Peaslee's treatment these two cross sections should be as observed for the lower energies and tend toward the same value at high energies. As will be explained presently there is an ambiguity in the interpretation of these

curves which does not allow one to rule out the validity of Peaslee's prediction. For the moment, let us consider the curves at their face value. Peaslee considers that the bulk of the (d,n) and (d,p) reaction arise from a stripping process in which either the proton or the neutron is captured by the nucleus while the other misses and continues on its way. Furthermore, it is assumed that this stripping process only takes place if the nucleon captured has essentially zero or negative energy which can be visualized as occurring by a favorable partitioning of internal energy of deuterons governed by its internal wave function such that the nucleon which is not captured carries off energy equal to or in excess of the incident energy of the deuteron. The reasoning is that if a nucleon is captured with positive energy the nucleus will be sufficiently excited to lose a neutron promptly thus resulting in a (d,pn) or (d,2n) reaction. This condition is probably unnecessarily restrictive since it is well known that radiative capture processes can occur with appreciable cross section with neutrons of energy well above zero.[7] With regard to expectations of the cross sections at high energies according to Peaslee's treatment, one might expect that the (d,p) and (d,n) cross sections would tend toward the same value. However, if one will allow radiative capture to compete with other reactions when the captured nucleon has positive energy of the order of one to several Mev, then it can be seen that the (d,p) reaction would be less prominent than the (d,n) reaction. For the (d,p) reaction, some yield could be lost as suggested by Peaslee by the captured neutron of positive energy undergoing an elastic or inelastic collision and then leaving. However,

a captured proton((d,n) reaction) with only a few Mev positive energy would not be eligible to leave because of the potential barrier and would of necessity give up its energy to the nucleus, after which we might admit radiation to compete with neutron emission.

At first sight, it might appear from Figure 1 that the mechanism postulated is confirmed because at high incident deuteron energy the (d,n) cross section is about 3.5 times greater than the (d,p) cross section. However, there is doubt that the yield of RaE corresponds to the entire (d,p) cross section in view of the recent knowledge of the existance of an isomeric state of Bi^{210}.[8] Although at the present moment the yield of Bi^{210m} cannot be determined owing to its long half-life and small cross section, one might assume that the ratio of the yield of Bi^{210} to that of Bi^{210m} might be almost the same for any incident energy of the deuteron. If so, the (d,p) excitation curve in Figure 1 will be shifted up by a constant factor, g.

$$g = \frac{P_1 + P_2}{P_1}$$

where P_1 = yield of Bi^{210}

P_2 = yield of Bi^{210m}

Let us now compare the veriation with deuteron energy of the (d,p) and (d,n) cross sections at high energies with theoretical prediction, According to the derivation by Peaslee, the probability of forming a proton in the stripping process with energy, E_p, $E_d - I \leq E_p \leq E_d - I + E_o$, varies inversely with approximately $E_d^{3/2}$ for high deuteron

energies (100 - 180 Mev), where I is the binding energy of the deuteron and E_o is the maximum binding energy of the neutron in residual nucleus.

Examining our data together with Kelly and Segrè's by plotting the log of (d,p) cross section against the log of E_d, the slope of the curve (see Figure 9) is approximately -1.5 in the energy region of 14 to 60 Mev in fair agreement with prediction, but decreases gradually to about -4.0 as E_d increases to 180 Mev. (It would be also true for (d,p) excitation curve including both the yield of Bi^{210} and Bi^{210m} if we assume g is a constant for all E_d.)

The same is true for (d,n) reaction with E_d above 80 Mev, the slope of the curve plotting log of cross section against the log of E_d decreases approximately from -1.5 to -4.0 as E_d increases from 80 to 180 Mev.

In conclusion it appears that the treatment of (d,p) and (d,n) reactions at low energies by Peaslee is not directly applicable at the high energies, for the experimentally observed cross sections decrease with energy above 100 Mev much more rapidly than the Peaslee expression indicates. It seems probable that the sticking probabilities ξ_p and ξ_n are decreasing functions of the energy in the high energy region. A theoretical treatment of the high energy reaction should probably be made in an analogous manner to that employed by Chew and Goldberger[10] on the inverse (n,d) and (p,d) reactions.

The (d,3n), (d,5n) reactions can be considered to proceed in both ways: (1) direct absorption of a deuteron and subsequent evaporation of three or five neutrons, and (2) absorption of a proton during the

stripping reaction followed by evaporation of two or four neutrons. The (α,2pn), (α,3n), (α,p2n), (α,p4n), and (α,p6n) reactions are likely to be due to the formation of compound nucleus followed by the evaporation of right number of nucleons, although (α,2pn) and (α,p2n) reactions can equally adequately be considered to proceed by the absorption of a neutron or proton in a zero or negative energy state or with a positive energy up to several Mev due to the relative motion of the proton or neutron inside the helium ion with respect to the center of the mass of that helium ion.

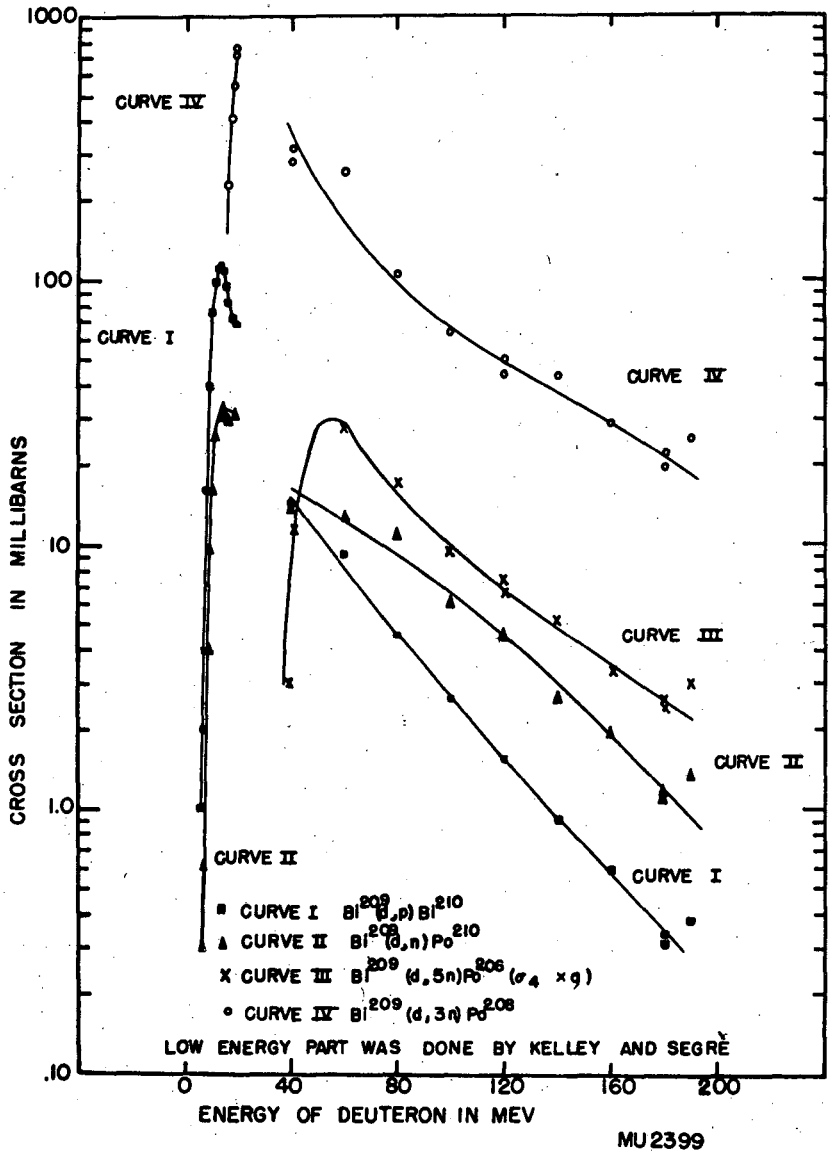

Figure 1

Part I

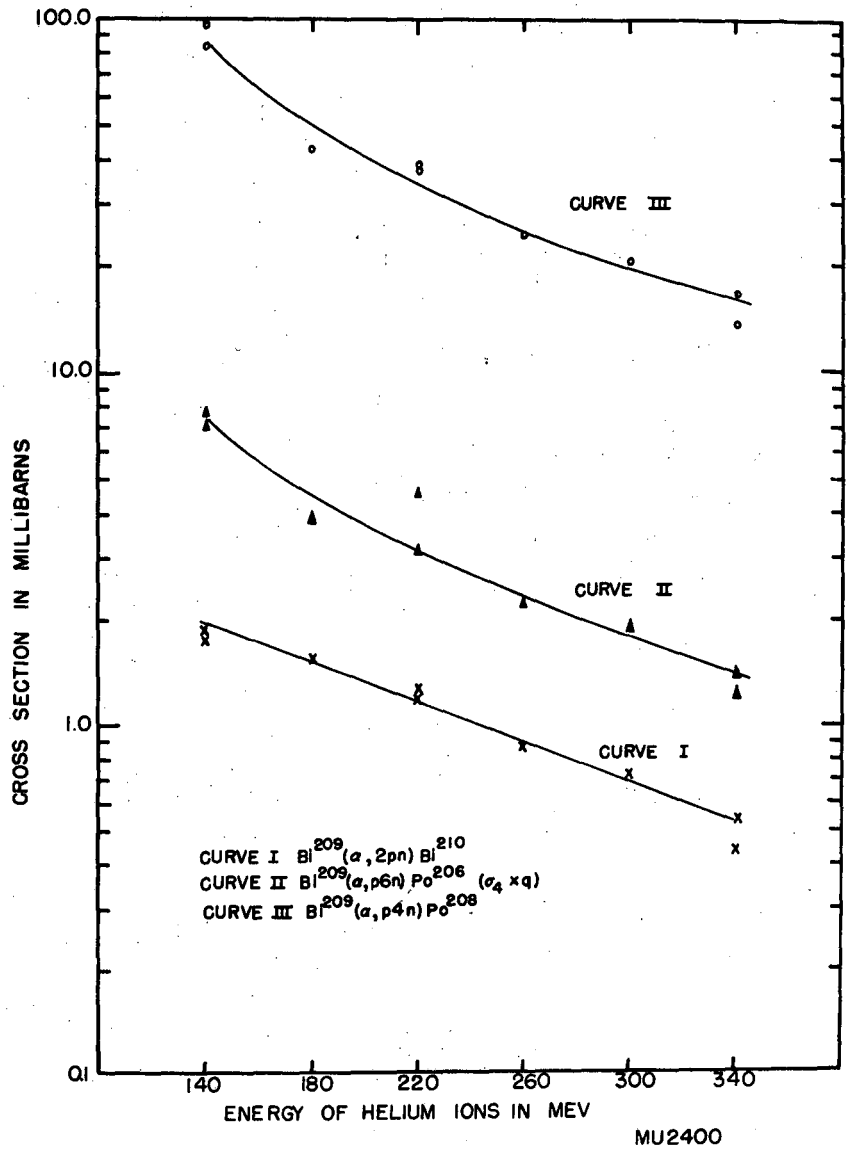

Figure 2

Part I

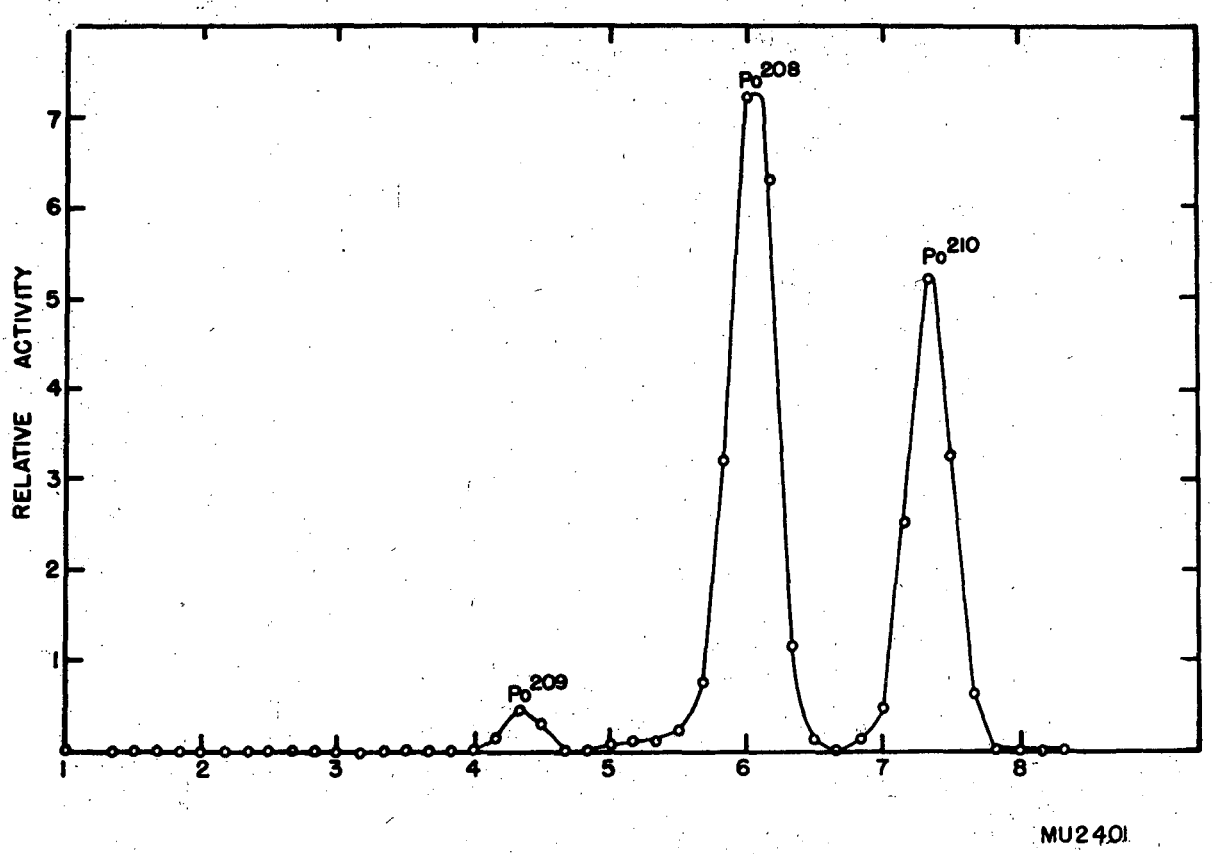

Figure 3

Part I

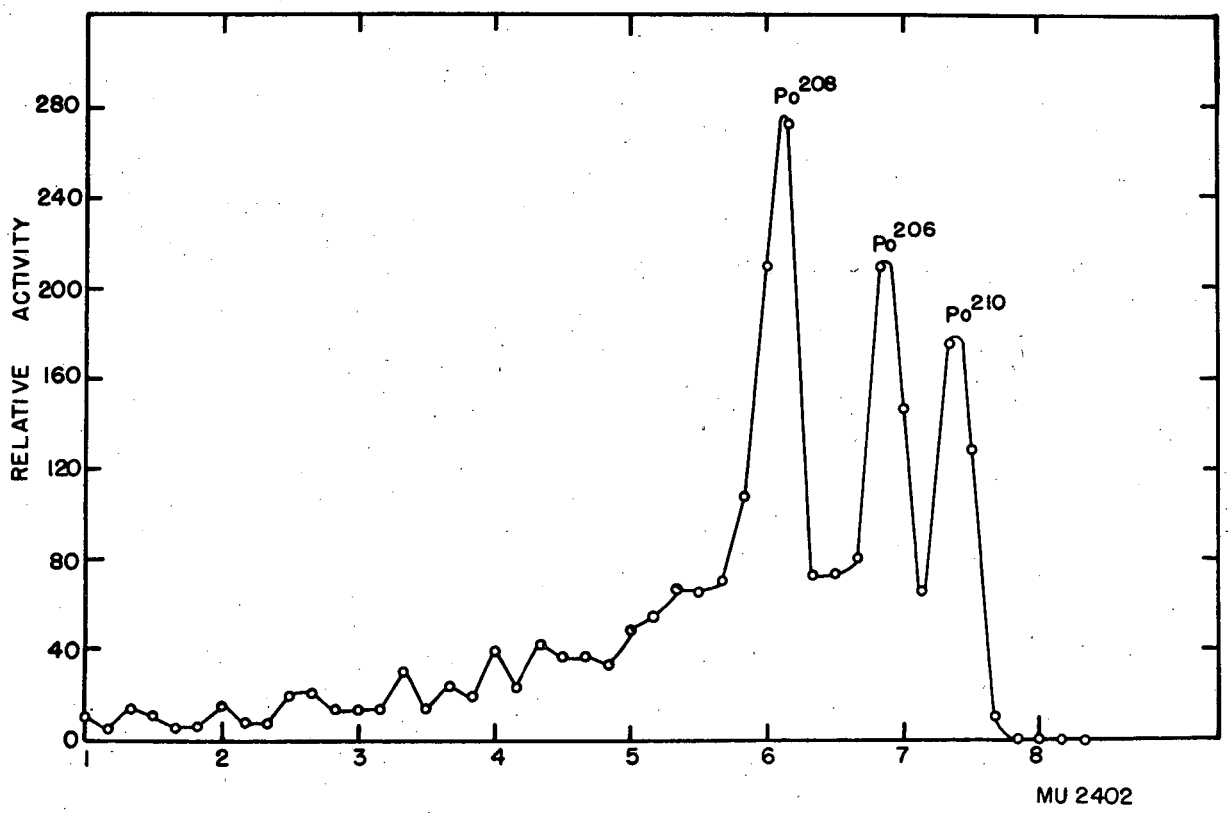

Figure 4

Part I

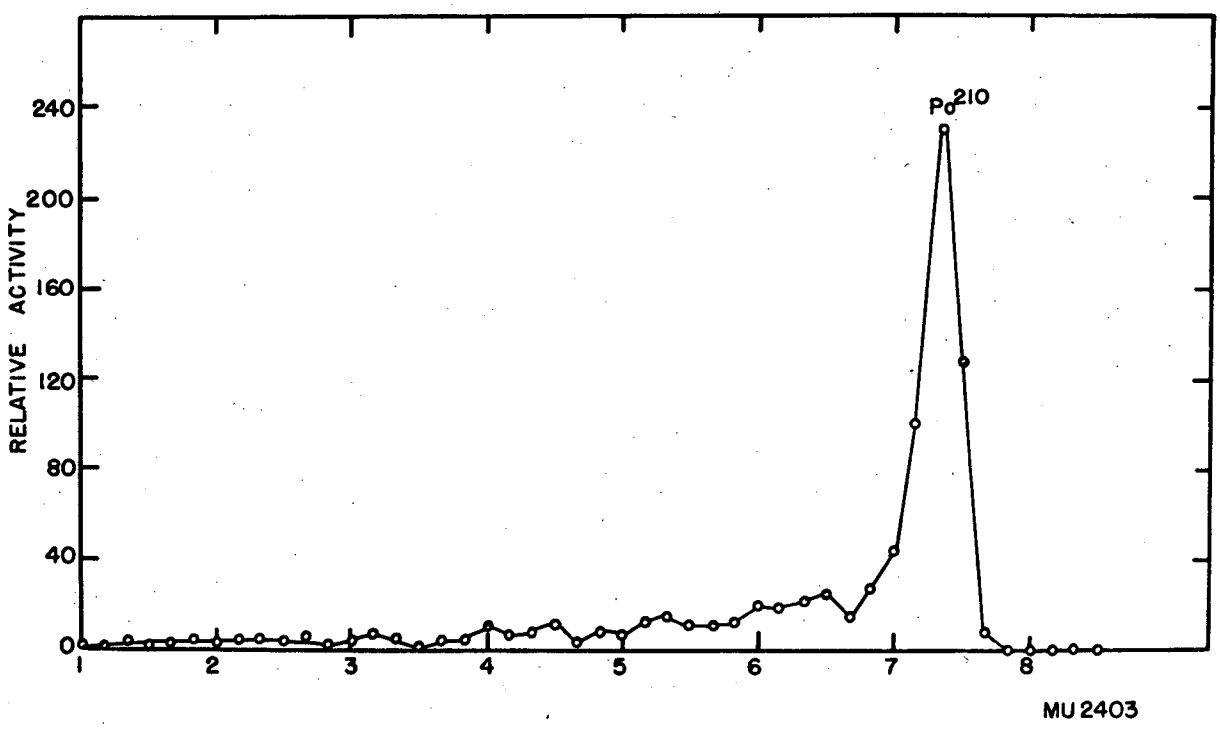

Figure 5

Part I

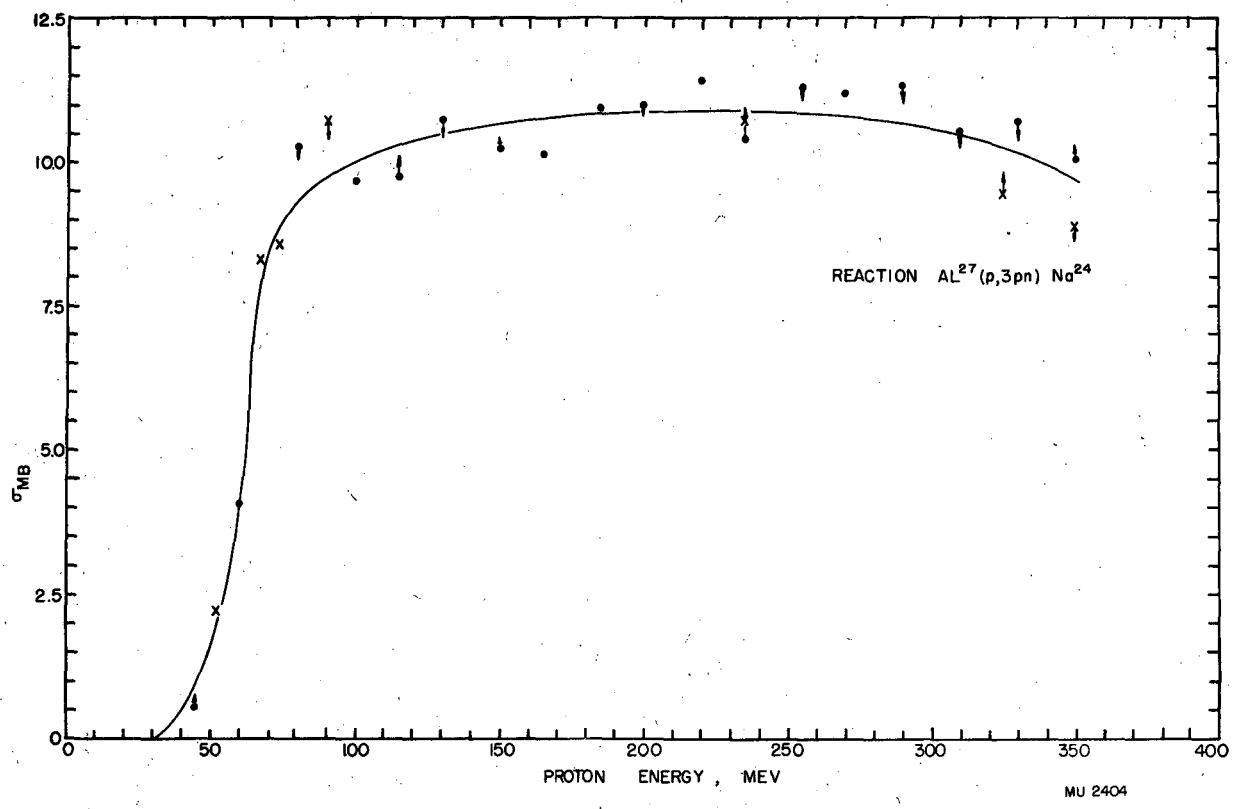

Figure 6

Part I

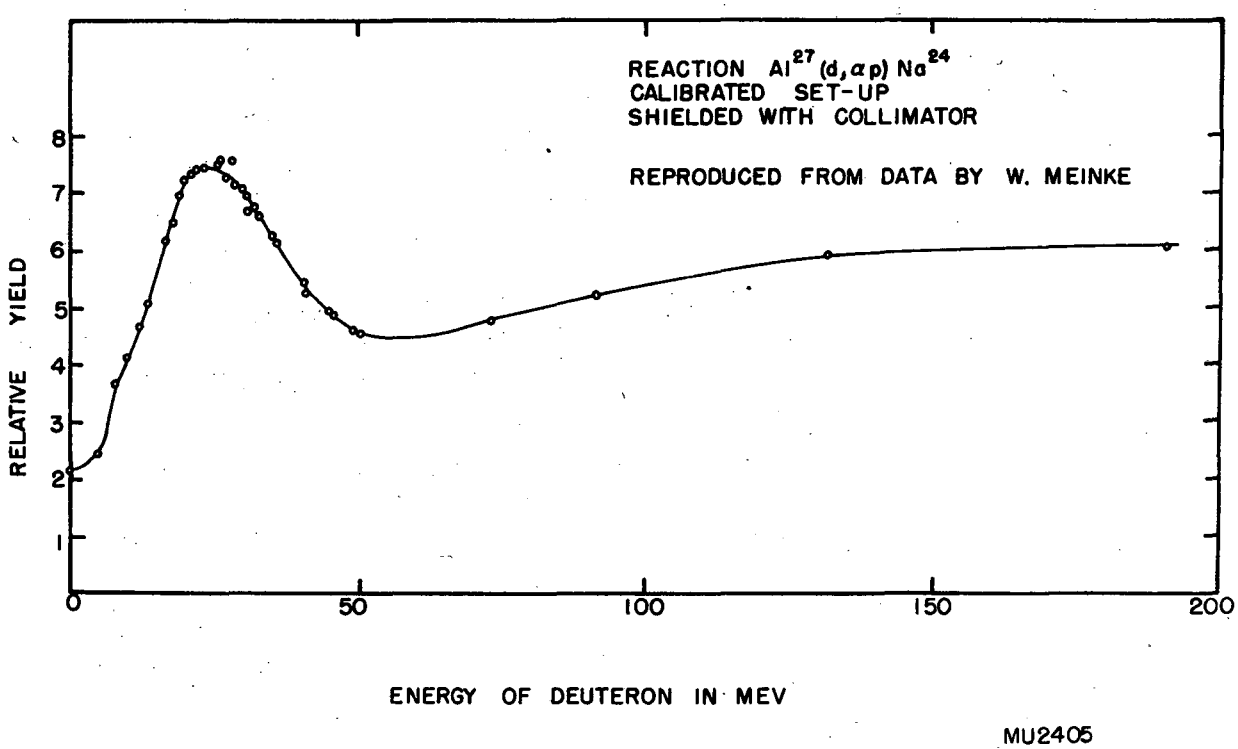

Figure 7

Part I

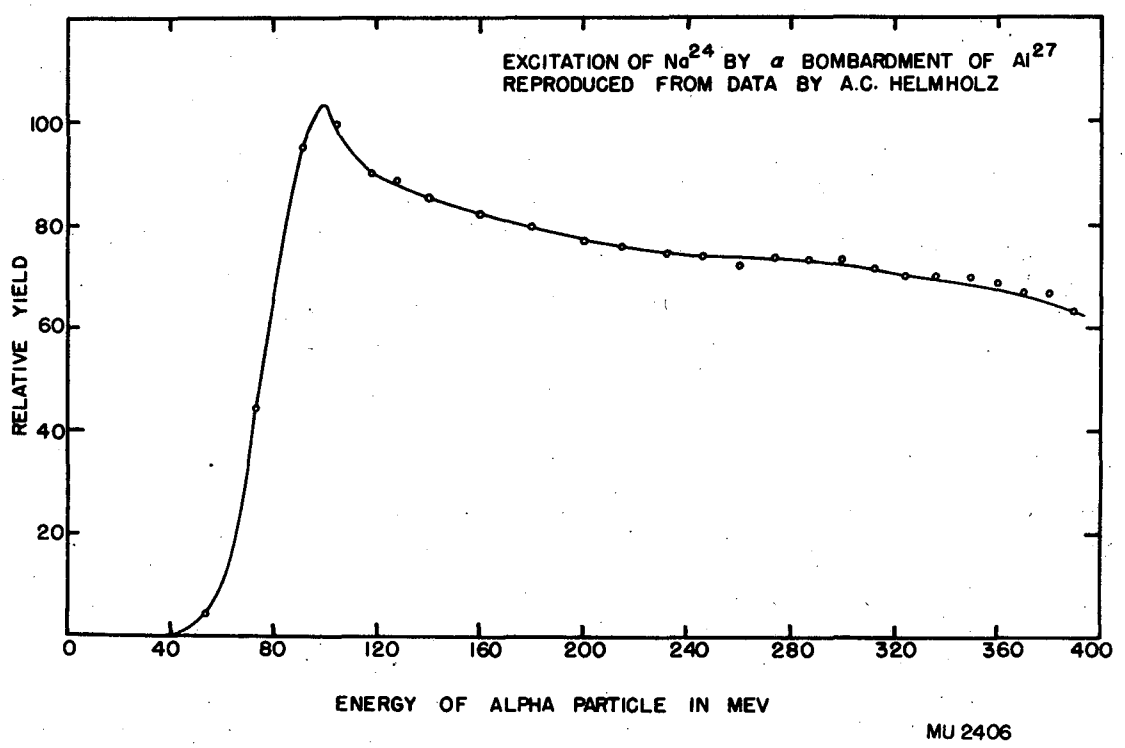

Figure 8

Part I

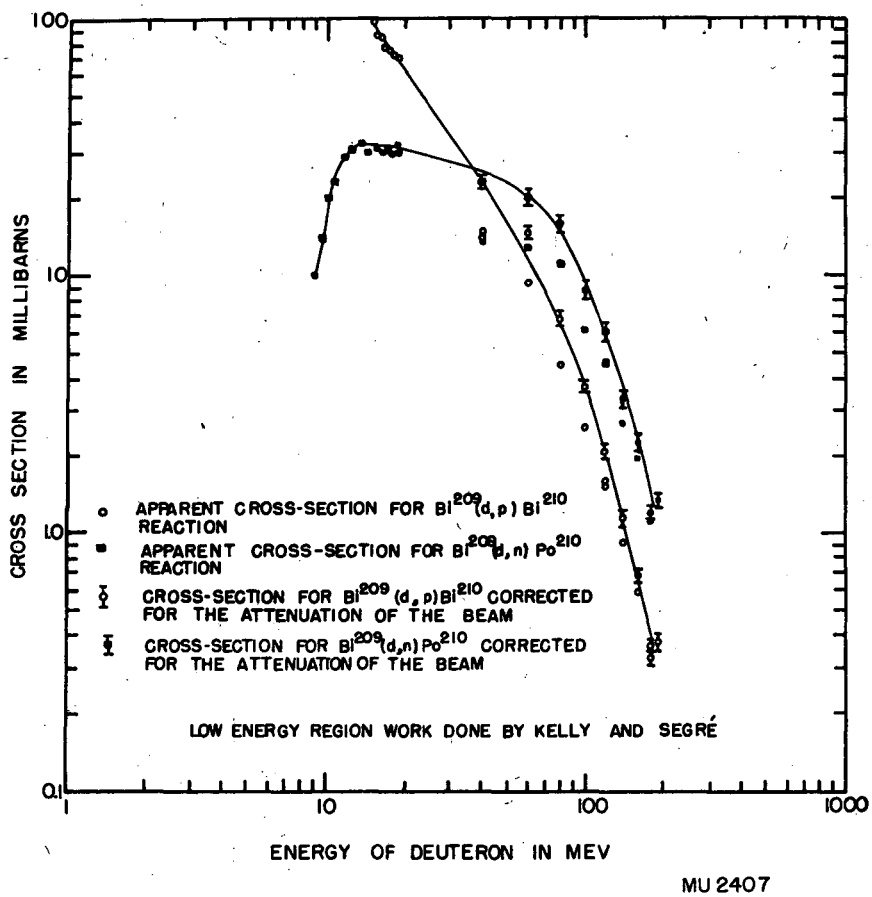

Figure 9

Part I

V. REFERENCES

1. E. L. Kelly and E. Segrè, Phys. Rev. 75, 999 (1949).
2. D. C. Peaslee, ibid., 74, 1001 (1948).
3. A. C. Helmholz, private communication.
4. A. Ghiorso, A. H. Jaffey, H. P. Robinson, and B. B. Weissbourd, "An Alpha Pulse Analyzer Apparatus," NNES PPR 14B, Paper 17.3 (1949).
5. P. C. Stevenson and R. L. Folger, private communication.
6. V. Peterson and R. Phillips, private communication.
7. D. J. Hughes, W. D. B. Spatz, and N. Goldstein, Phys. Rev. 75, 1781 (1949).
8. H. M. Neumann, J. J. Howland, Jr., and I. Perlman, Phys. Rev. 77, 720 (1950).
9. R. Serber, ibid. 72, 1008 (1947).
10. G. F. Chew and M. L. Goldberger, ibid. 77, 470 (1950).

Table of Contents (Part II)

		Page
I.	INTRODUCTION.	41
II.	THEORY.	42
III.	EXPERIMENTAL.	45
IV.	CALCULATION AND RESULTS	46
V.	DISCUSSION	53
VI.	CONCLUSION	54
VII.	ACKNOWLEDGMENTS.	55
VIII.	APPENDIX	56
	FIGURES	57
IX.	REFERENCES	61

List of Figures (Part II)

Figure 1. A diagram of angular dependence of the momentum of recoil Na^{24} with the assumption of the compound nucleus model.

Figure 2. Percentage of recoil loss of Na^{24} from the first aluminum foil of 0.00025 inch thick by bombarding with protons of various energies.

Figure 3. Percentage of recoil loss of Na^{24} from the first aluminum foil of 0.00025 inch thick by bombarding with deuterons of various energies.

Figure 4. Percentage of recoil loss of Na^{24} from first aluminum foil of 0.0005 inch thick by bombarding with alpha particles of various energies.

Figure 5. A graph for the calculation of percentage of recoil loss of Na^{24} from the first aluminum foil with the assumption of the compound nucleus model.

Part II

RECOIL OF Na^{24} PRODUCED IN ALUMINUM FOIL BY BOMBARDMENT WITH HIGH ENERGY NUCLEAR PARTICLES

I. INTRODUCTION

Since the successful operation of the Berkeley 184-inch synchro-cyclotron, a great deal of work about the nuclear reactions induced by high energy nuclear particles has been performed. A striking feature of numerous nuclear reactions of this type is the slow variation of excitation function with energy of incident particles.

Serber[1] proposed that the above phenomenon, which can no longer be satisfactorily explained by the compound nucleus formation as postulated by Bohr, is mainly due to the reason that the reaction occurs through the incident particle carrying off a good fraction of its energy and gives the nucleus approximately the right amount of excitation energy for the reaction to proceed.

During our investigation of excitation function of $(\alpha,\alpha 2pn)$ reaction on bismuth, it was discovered that the amount of $_{11}Na^{24}$ produced in the first aluminum foil is less than that in the following foils which were all used as monitors in determining the beam intensity inside the Berkeley 184-inch cyclotron. It was of interest to us to determine the cause of this effect. Through the experimental arrangements and results obtained, which will be described in following sections, the loss of Na^{24} activity of the first aluminum foil due to recoil and its dependence on energy of incident particles constitute a solid proof of Serber's

mechanism for the high energy region, while compound nucleus model apparently can account for the low energy part.

The purpose of this investigation is to determine the energy dependence of recoil of Na^{24} with a desire of clarifying the picture of high energy nuclear reactions.

II. THEORY

According to the theory of compound nucleus, the mechanism of reactions can be formulated as follows:

$$_{13}Al^{27} + {}_{2}He^{4} \longrightarrow {}_{15}P^{31*} \longrightarrow {}_{11}Na^{24} + n + 2\,{}_{1}H^{1} + {}_{2}He^{4} \qquad (1)$$

$$_{13}Al^{27} + {}_{1}H^{1} \longrightarrow {}_{14}Si^{28*} \longrightarrow {}_{11}Na^{24} + n + 3\,{}_{1}H^{1} \qquad (2)$$

$$_{13}Al^{27} + {}_{1}H^{2} \longrightarrow {}_{14}Si^{29*} \longrightarrow {}_{11}Na^{24} + {}_{1}H^{1} + {}_{2}He^{4} \qquad (3a)$$

$$_{13}Al^{27} + {}_{1}H^{2} \longrightarrow {}_{14}Si^{29*} \longrightarrow {}_{11}Na^{24} + {}_{1}H^{2} + n + 2\,{}_{1}H^{1} \qquad (3b)$$

$$_{13}Al^{27} + {}_{1}H^{2} \longrightarrow {}_{14}Si^{28*} + n \longrightarrow {}_{11}Na^{24} + 2n + 3\,{}_{1}H^{1} \qquad (3c)$$

$$_{13}Al^{27} + {}_{1}H^{2} \longrightarrow {}_{13}Al^{28*} + {}_{1}H^{1} \longrightarrow {}_{11}Na^{24} + {}_{1}H^{1} + {}_{2}He^{4} \qquad (3d)$$

In case of $_{2}He^{4}$ ion bombardment, by conservation of momentum, $_{15}P^{31*}$ has a momentum vector $\vec{P}$ in forward direction $\vec{k}$ which can be calculated:

$$\vec{P} = \sqrt{2M_{\alpha}E_{o}}\ \vec{k}$$

where E_o is energy of incident particle M_{α}, mass of an alpha particle. The subsequent evaporation of one neutron, one alpha particle and two protons can be treated as a random walk like problem.

The momentum $|\vec{P_1}|$ (oriented equally probably in all directions) acquired by the resultant $_{11}Na^{24}$ due to evaporation is then:

$$|\vec{P_1}| \cong \left(\sum_{i=1}^{4} p_i^2\right)^{1/2} \ldots\ldots \tag{4}$$

where p's are the momenta of the evaporated particles. With pretty good approximation by assuming evaporation under constant temperature of nucleus, $|\vec{P_1}|$ can be expressed in terms of energy of incident particle (E_o), potential barrier of the compound nucleus towards protons (V) and the average binding energy (B) of nucleons inside the nucleus.

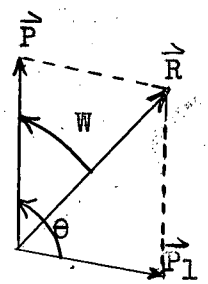

Figure 1.

$$|\vec{P_1}| \cong \frac{0.97}{\sqrt{2}} \left\{ \frac{M_{Al}}{M_{Al} + M_\alpha} (M_n + 2M_p + M_\alpha)E_o - 3(M_n + 2M_p + M_\alpha)B + 4(M_\alpha - M_n)V \right\}^{1/2} \tag{5}$$

From Figure 1 we can easily express $|\vec{R}|$ and W as functions of the variable θ.

$$|\vec{R}| = \sqrt{\vec{P}^2 + \vec{P_1}^2 + 2|\vec{P}|\,|\vec{P_1}|\cos\theta} \tag{6}$$

$$W = \tan^{-1} \frac{|\vec{P_1}| \sin \theta}{|\vec{P}| + |\vec{P_1}| \cos \theta} \tag{7}$$

From resultant momentum $|\vec{R}|$, the range of Na^{24} in aluminum can be calculated by applying the theory developed by Bohr,[2] and Knipp and Teller[3] together with value of atomic stopping power of aluminum listed by Livingston and Bethe.[4]

The fraction of loss of Na^{24} from the first foil can be obtained from the following integration.

$$f = \frac{1}{2t} \int_0^{\pi} s \cos w \sin \theta \, d\theta \tag{8}$$

where t is the thickness of aluminum foil, and s is the range of the Na^{24} ion both in $MgCm^{-2}$ of aluminum.

In case of proton bombardment, the forward momentum $\vec{P}$ of ${}_{14}Si^{28*}$ due to compound nucleus formation is

$$\vec{P} = \sqrt{2M_p E_o} \; \vec{k}$$

The momentum $|\vec{P_1}|$ acquired by the resultant ${}_{11}Na^{24}$ due to evaporation off one neutron and three protons can be shown to be:

$$|\vec{P_1}| \approx \frac{0.98}{\sqrt{2}} \left\{ \frac{M_{Al}}{M_{Al} + M_P} (M_n + 3M_P)E_o - 3(M_n + 3M_P)B + 3(M_P - M_n)V \right\}^{1/2} \tag{9}$$

The symbols are of same significance as before. The fraction of loss of Na^{24} from the first foil can again be obtained from equation (8).

Since the situation is complicated by the fact that the reaction may take place through several paths, this treatment will not be extended

to the deuteron bombardment. The purpose of this theoretical treatment is to verify the statement that the compound nucleus model can account for the nuclear reaction with low energy incident particles as well as Serber's mechanism for the high energy ones by comparing the experimental data with the calculated values.

III. EXPERIMENTAL

A standard procedure of the experiment is as follows: Four to six layers of aluminum foils of the same thickness sandwiched by two or more sheets of 10 mil graphite or 5 mil polystyrene were mounted in a clamp type target holder. The edges of the rectangular shaped foil were flush with one another. After the bombardment (7 - 30 minutes) the foils were cut into equal and corresponding areas. After approximately 15 hours, all the foils were weighed and mounted separately on the same type scotch-tape counting plates and counted every four to eight hours for approximately 60 hours on the same shelf of the same Geiger-Müller counter. The activities of different foils were plotted against time on a three cycle semilog paper. The points in an interval of more than 45 hours lie close to within one percent on a line of 15 hours half-life of Na^{24}. The activities of Na^{24} in different foils at the same instant were then compared. The aluminum foils contained almost the same amount of Na^{24} activity except the first one which always has much lower amount of Na^{24} activity than the others. (In case of ${}_2He^4$ ion bombardment with energy ranging from 80 - 160 Mev, the second foil has lower activity than the 3rd and 4th foils by 2 - 5 percent due to the small fraction of recoil

Na^{24} with range greater than the thickness of the aluminum foil.) The graphite or polystyrene layer right behind the aluminum foil catches almost quantitatively the amount of Na^{24} the first aluminum foil loses, whereas the graphite or polystyrene in front of the aluminum foils catch a small amount or no activity.

Therefore it can be safely concluded that this phenomenon is due to the recoil of the Na^{24} produced in aluminum foils by the incident particles, and the range of the Na^{24} recoil particles in aluminum with several exceptions (see nearest parenthesis above) is less than the thickness of the foil.

IV. CALCULATION AND RESULTS

The percentage of recoil loss of Na^{24} in the first aluminum foil can be calculated as follows:

$$L = 100\left(1 - \frac{A_1 \bar{W}}{\bar{A} W_1}\right)$$

where A_1 = activity of Na^{24} in first aluminum foil at certain instant t

$\bar{A}$ = average activity of Na^{24} in other aluminum foils at same instant t (in case of the bombardments with 80 - 160 Mev alpha particles on the 0.00025 inch thick aluminum foils the average activity of Na^{24} in the third and fourth aluminum foils were used).

W_1 = weight of first aluminum foil

$\bar{W}$ = average weight of the other aluminum foils.

The difference in the weight of different aluminum foils in each bombardment was within one percent.

The Na^{24} activity caught in graphite or polystyrene right behind the aluminum foils (C_f) and that caught in graphite or polystyrene in front of the aluminum foils (C_b) were calculated as follows:

$$C_f = \frac{100\ A_f}{\overline{A}}$$

$$C_b = \frac{100\ A_b}{\overline{A}}$$

where A_f = activity of Na^{24} in graphite or polystyrene right behind the aluminum foils at time t.

A_b = activity of Na^{24} in graphite or polystyrene in front of the aluminum foils at time t.

The results of the experiments are summarized in Table I. The alpha and deuteron beam inside the cyclotron are mutually contaminated, especially when we run alpha beam right after the deuterom beam or vice versa. The low values of percentage of loss due to recoil for 60 Mev and 90 Mev alpha particles were mainly due to this reason as well as the lower cross section for $Al^{27}(\alpha,\alpha 2pn)Na^{24}$ reaction in comparing with that of $Al^{27}(d,\alpha p)Na^{24}$ and $Al^{27}(d,d2pn)Na^{24}$ reactions with deuteron energy half of that of alpha particles (reference 3, Part I). The ratio of alpha to deuteron was roughly estimated to be 15 to 1 before the experiments, 38, 39, 50, 51, 60, 61, 64, 65 were carried out. The values of percentage of loss due to recoil for 80 Mev will be shown later to be reasonably close to the calculated value with the assumption of compound nucleus model.

Table I

Experiment number	Nuclear particles	Energy of particle (Mev)	Thickness of Al foils (inches)	Percent of loss of Na^{24} of first Al foil	Percent of catching of Na^{24} in graphite or polystyrene* right behind the Al foils	Percent of catching of Na^{24} in graphite or polystyrene* in front of Al foils
1	proton	60	0.00025	27.8	28.0	<2.0
2	proton	60	0.00025	26.4	28.3	<2.2
3	proton	70	0.00025	29.2	29.0	<1.5
4	proton	80	0.00025	27.3	25.4*	<0.6*
5	proton	80	0.00025	28.5	25.1*	<0.4*
6	proton	90	0.0005	12.9	13.2	
7	proton	90	0.00025	26.8	26.2	<2.0
8	proton	140	0.00025	20.9	19.9	
9	proton	180	0.00025	18.2	18.2*	≳1.7*
10	proton	180	0.00025	18.6	18.0*	~1.5*
11	proton	220	0.00025	17.6	17.6	
12	proton	280	0.00025	17.5	16.4	
13	proton	340	0.0005	7.6	7.6	<<2.0
14	proton	340	0.00025	15.0	15.7	<<4.0
15	proton	340	0.00025	16.3	17.1	<<4.0
16	proton	340	0.00025	15.5	14.4*	~2.6*
17	proton	340	0.00025	13.9	14.5*	~2.8*
18	deuteron	40	0.00025	22.2		
19	deuteron	60	0.00025	25.8	28.0	<2.5
20	deuteron	60	0.0005	12.0	12.6	<1.3
21	deuteron	80	0.00025	32.4	34.1	<2.6
22	deuteron	80	0.0005	17.0	14.8	<1.3
23	deuteron	100	0.00025	32.0	32.2*	~1.0*
24	deuteron	100	0.0005	17.3	15.5*	~0.7*
25	deuteron	120	0.00025	30.8	28.2*	~1.0*
26	deuteron	120	0.0005	16.2	13.5*	~0.5*
27	deuteron	140	0.0005	15.5		
28	deuteron	160	0.00025	27.0	27.4*	~1.3*

Table I (continued)

Experiment number	Nuclear particles	Energy of particle (Mev)	Thickness of Al foils (inches)	Percent of loss of Na^{24} of first Al foil	Percent of catching of Na^{24} in graphite or polystyrene* right behind the Al foils	Percent of catching of Na^{24} in graphite or polystyrene* in front of Al foils
29	deuteron	160	0.00025	27.4	26.8*	~1.3*
30	deuteron	190	0.00025	25.0	23.8*	~1.3*
31	deuteron	190	0.00025	24.8	24.6*	~1.2*
32	deuteron	194	0.00025	26.6	26.8	
33	deuteron	194	0.0005	12.4		
34	deuteron	194	0.0005	12.7		
35	deuteron	194	0.001	6.4		<0.05
36	alpha	60	0.00025	23.5	23.6	<0.7
37	alpha	60	0.00025	24.2	21.4	<0.7
38	alpha	80	0.00025	57.8	64.8	<1.7
39	alpha	80	0.00025	59.0	65.2	<1.7
40	alpha	90	0.00025	28.1	30.3	<1.1
41	alpha	90	0.00025	29.4	28.5	<1.1
42	alpha	90	0.00025	38.0	36.2	<1.7
43	alpha	90	0.00025	36.0	36.9	<1.8
44	alpha	100	0.00025	59.7	64.6	<1.0
45	alpha	100	0.0005	29.4	30.2	<0.5
46	alpha	110	0.00025	60.3	67.6	<1.0
47	alpha	110	0.00025	61.9	68.5	<1.0
48	alpha	120	0.00025	58.7	62.3	<1.1
49	alpha	120	0.0005	32.7	30.0	<0.6
50	alpha	120	0.00025	60.3	68.1	<1.9
51	alpha	120	0.00025	58.7	66.5	<1.9
52	alpha	130	0.00025	56.4	66.0	<1.7
53	alpha	130	0.00025	56.8	67.4	<1.7
54	alpha	140	0.0005	27.5		
55	alpha	140	0.0005	27.1	26.0	
56	alpha	140	0.00025	54.2	59.3	<1.3
57	alpha	140	0.0005	27.8	28.2	<0.7

Table I (continued)

Experiment number	Nuclear particles	Energy of particle (Mev)	Thickness of Al foils (inches)	Percent of loss of Na^{24} of first Al foil	Percent of catching of Na^{24} in graphite or polystyrene* right behind the Al foils	Percent of catching of Na^{24} in graphite or polystyrene* in front of Al foils
58	alpha	160	0.00025	50.5	59.3	<1.9
59	alpha	160	0.00025	51.3	60.7	<1.9
60	alpha	190	0.00025	46.2	55.7	<2.8
61	alpha	190	0.00025	48.2	54.3	<2.0
62	alpha	220	0.00025	35.0	34.1	<1.8
63	alpha	220	0.00025	34.8	35.1	<1.8
64	alpha	280	0.00025	35.6	41.9	<6.0
65	alpha	280	0.00025	35.9	43.1	<2.9
66	alpha	340	0.0005	16.6		<1.5
67	alpha	340	0.0005	14.9		<1.5
68	alpha	340	0.0005	16.7		<1.5
69	alpha	340	0.00025	27.7	29.8	<2.5
70	alpha	340	0.00025	26.7	31.0	<2.2
71	alpha	370	0.0005	13.0		<0.9
72	alpha	370	0.0005	14.0		<1.0
73	alpha	370	0.0005	14.9		<1.2
74	alpha	380	0.00025	24.2		

Fortunately, for the bombardments with high energy alpha particles (above 220 Mev), the percentage of loss due to recoil is about the same as that with deuterons of half the amount of energy. Therefore the error due to the contamination in this region should be less than two percent for the 0.00025 inch foils. In case of using polystyrene as catcher of the recoiled Na^{24}, the beam intensity inside the cyclotron was cut to 0.06 to 0.10 of the maximum intensity in order to avoid melting of polystyrene during bombardment.

The calculated percentage of loss of Na^{24} of the first aluminum foil for several energies of proton and helium ions with the assumption of the compound nucleus model will be compared with the experimental value in Table II.

Table II

Nuclear Particles	Energy of particle (Mev)	Thickness of Al foils (inches)	Percent of loss of Na^{24} of first Al foil (expl.)	Percent of catching of Na^{24} in graphite or polystyrene behind the Al foils	Calculated percent of loss of Na^{24} of first Al foil Knipp-Teller's Theory $\gamma^* = 1.3$	Knipp-Teller's Theory $\gamma = 1.4$	Bohr's Theory $\gamma = 1$
proton	60	0.00025	27.1	28.2	33.5	28.1	18.8
proton	70	0.00025	29.2	29.0	35.5	29.8	20.5
proton	80	0.00025	27.9	25.3	36.5	31.2	21.8
proton	140	0.00025	20.9	19.9	48.1	42.3	30.2
proton	180	0.00025	18.4	18.1	57.0	51.1	36.0
proton	340	0.00025	14.7	14.5	97.3	90.0	66.9
alpha	80	0.0005	29.2**	32.5	37.5	34.3	24.4
alpha	100	0.0005	29.4	30.2	45.5	41.3	30.1
alpha	120	0.0005	32.7	30.0	54.5	49.9	36.6
alpha	140	0.0005	27.8	28.2	63.5	58.3	43.8

*$\gamma = V_e/V$ where V_e is the root mean square velocity of the energetically most easily removable electron which is determined from the Thomas-Fermi model, V is the volocity of the ion.

**Converted from percent of recoil loss of 0.00025 by dividing the value by 2.

V. DISCUSSION

The results show the dependence of percentage of loss due to recoil of Na^{24} in forward direction or its range upon the energy of the incident particles. In the case of proton and helium ions (see Figures 2 and 4), starting from the low energy side, the percentage of recoil loss which checks reasonably well with calculated values (using Bruning, Knipp, and Teller's theory and setting $\gamma = V_e/V = 1.4$), increases as the energy of incident particles increases, which is consistent with compound nucleus formation as postulated by Bohr. The percentage of recoil then passes through a maximum and decreases as the energy of incident particle increases. Therefore it clearly shows that the high energy incident particle transfers only part of its energy to the target nucleus by making one or more collisions with the nucleon or nucleons inside as it passes through in these particular nuclear reactions.* The maximum

---

*The fact that the percentage of recoil decreases as the energy of the incident particle increases can be explained by a simple approximate calculation assuming that after transferring a definite amount of energy, E, to the target nucleus as it passes through, the incident particle leaves the nucleus without changing its direction. The forward momentum of the excited Al^{27} will be:

$$|\vec{P}| = \sqrt{2M_iE_o} - \sqrt{2M_i(E_o - E)} = \frac{\sqrt{2M_i}\,E}{\sqrt{E_o} + \sqrt{E_o - E}}$$

where E_o = energy of incident particle

M_i = mass of incident particle, and $E_o > E$

It is obvious that $|\vec{P}|$ decreases as E_o increases.

As $|\vec{P_1}|$ will be the same for any incident energy (since E is a constant), the resultant momentum or energy of the Na^{24} ion in any direction or the percentage of recoil loss will decrease as E_o increases which is certainly consistent with the experimental data. The experimental fact that the backward recoil gradually increases as E_o increases (shown in the proton case with polystyrene as catcher) should also be expected from the above calculation. More exact calculation needs the data on angular distribution of those recoil Na^{24}.

in the curve for the case of proton is around 70 Mev and that for alpha particle is approximately 110 Mev. In the case of deuteron (see Figure 3), starting from low energy side, 40 - 80 Mev, the reactions (3d)(3a)(3c)(3b) take place simultaneously probably with (3d) of the most and (3b) of the least importance, the percentage of recoil increases as energy of the incident particle increases. The broad peak from 80 Mev to 140 Mev is due to the fact that the target nucleus begins to be increasingly transparent to deuterons but still opaque toward protons of reaction (3c). As the energy goes up still higher, the target nucleus becomes transparent to both incident deuterons and protons from the stripping process. Therefore, the percentage of recoil decreases as energy increases.

VI. CONCLUSION

The conclusion can be drawn from the above experimental facts that the compound nucleus model can only be applied for the nuclear reactions with the comparatively low energy incident particles, whereas the high energy nuclear reactions of above type, as we already have discussed, can only be satisfactorily explained by Serber's mechanism.

VII. ACKNOWLEDGMENTS

The author wishes to thank Professor I. Perlman for his kind guidance and assistance throughout these experiments. It is also a pleasure to acknowledge the helpful discussions with Professor A. C. Helmholz, Dr. H. M. Neumann, Dr. R. E. Batzel, and Mr. John O. Rasmussen. The author is grateful to Messrs. J. T. Vale, L. Houser, and members of the 184-inch cyclotron operating staff for their cooperation in making the irradiations for these studies and Mr. H. Jaffe for his help in calculations.

VIII. APPENDIX

A sample calculation of percentage of loss of Na^{24} of the first aluminum foil for 70 Mev protons with the assumption of compound nucleus model will be shown as follows: The range of Na^{24} in aluminum was determined by using Bruning, Knipp, and Teller's theory and setting gamma equal to 1.4 together with the value of the atomic stopping power of aluminum listed by Livingston and Bethe.

The forward momentum due to compound nucleus formation is:

$$|\vec{P}| = (2 \times 1.60 \times 10^{-6} \times 1.67 \times 10^{-24} \times 70)^{1/2} = 1.934 \times 10^{-14} \text{gm cm sec}^{-1}$$

The random oriented momentum due to evaporation can be calculated by using equation (9) with the assumption of $B \cong 8$ Mev and $V \cong 4$ Mev.

$$|\vec{P_1}| \cong 1.526 \times 10^{-14} \text{gm cm sec}^{-1}.$$

In fact, a variation of ± 1 Mev in B and V will affect very little the final result. The following table will list the required values for numerical integration. (See Figure 5.)

Table III

θ	Energy of Na^{24} ion (Mev)	Range in Al in mg cm^{-2} (S)	Cos W	S Cos W Sin θ (mg cm^{-2} $radian^{-1}$)
0				0
$\pi/36$	9.30	0.88	1	0.0767
$\pi/18$	9.26	0.87	1	0.151
$\pi/9$	9.05	0.86	0.988	0.290
$\pi/6$	8.70	0.85	0.973	0.414
$\pi/4$	7.97	0.82	0.942	0.546
$\pi/3$	7.03	0.78	0.899	0.607
$5\pi/12$	5.91	0.72	0.847	0.589
$\pi/2$	4.73	0.66	0.786	0.519
$2\pi/3$	2.44	0.51	0.665	0.294
$3\pi/4$	1.98	0.42	0.624	0.185
$5\pi/6$	0.755	0.30	0.629	0.0944
π				0

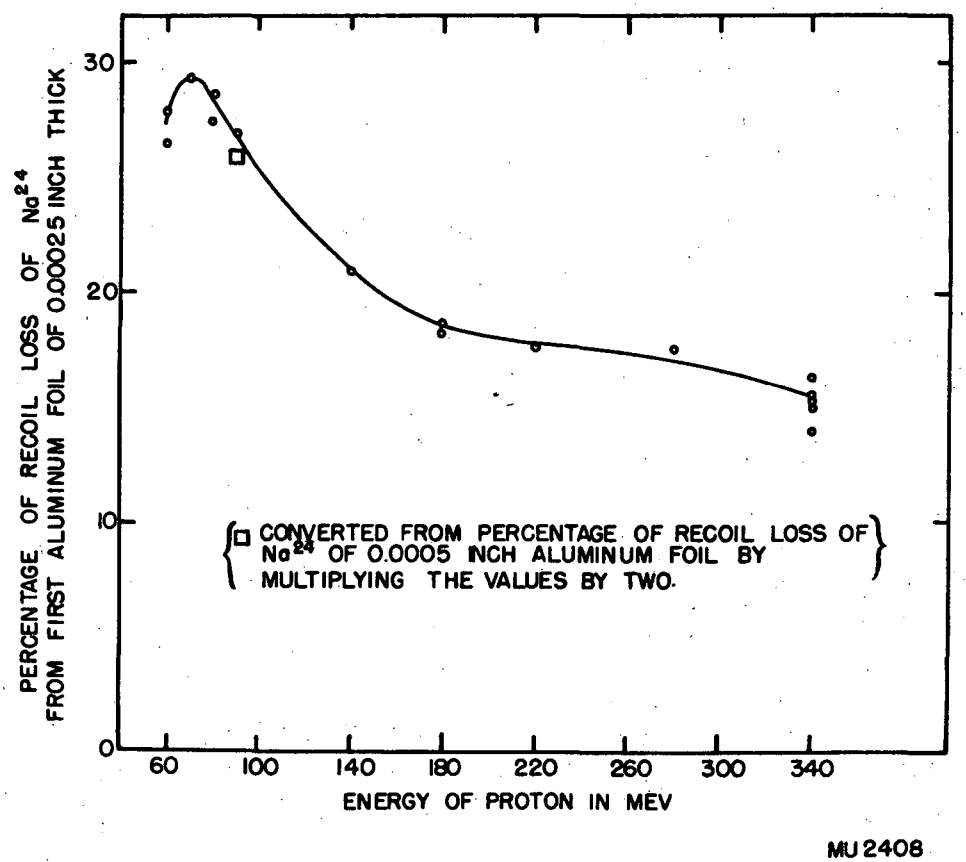

Figure 2

Part II

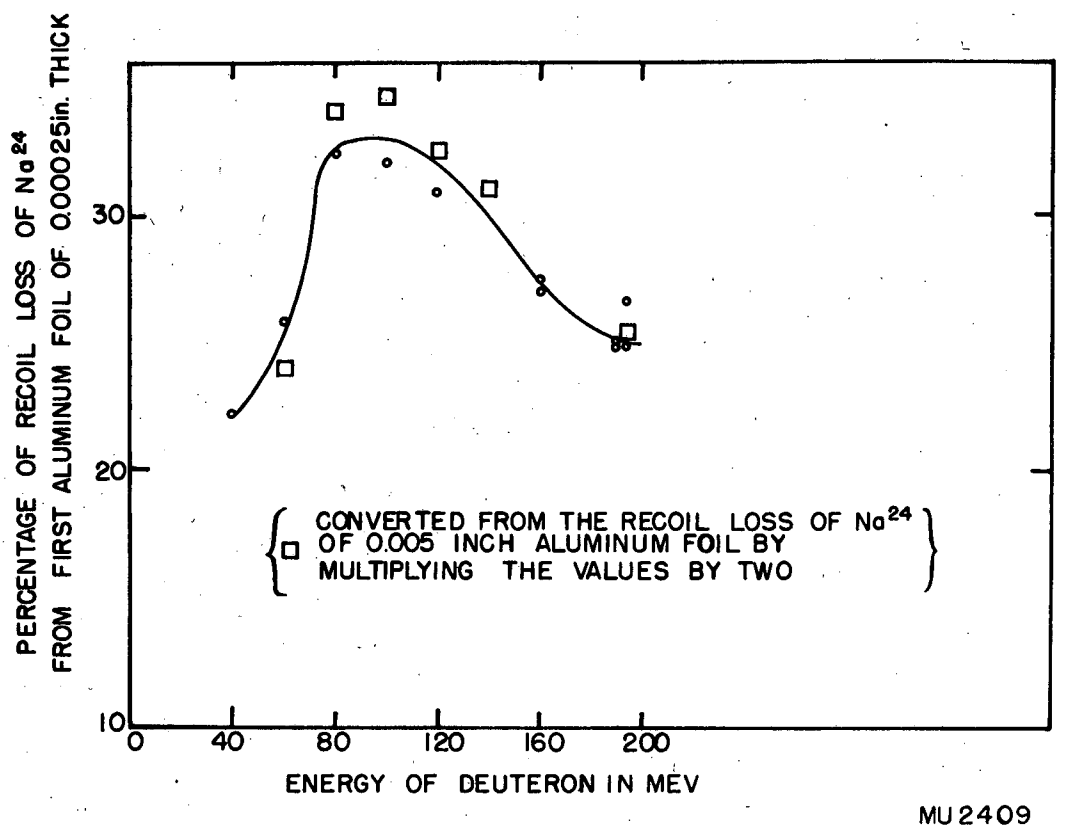

Figure 3

Part II

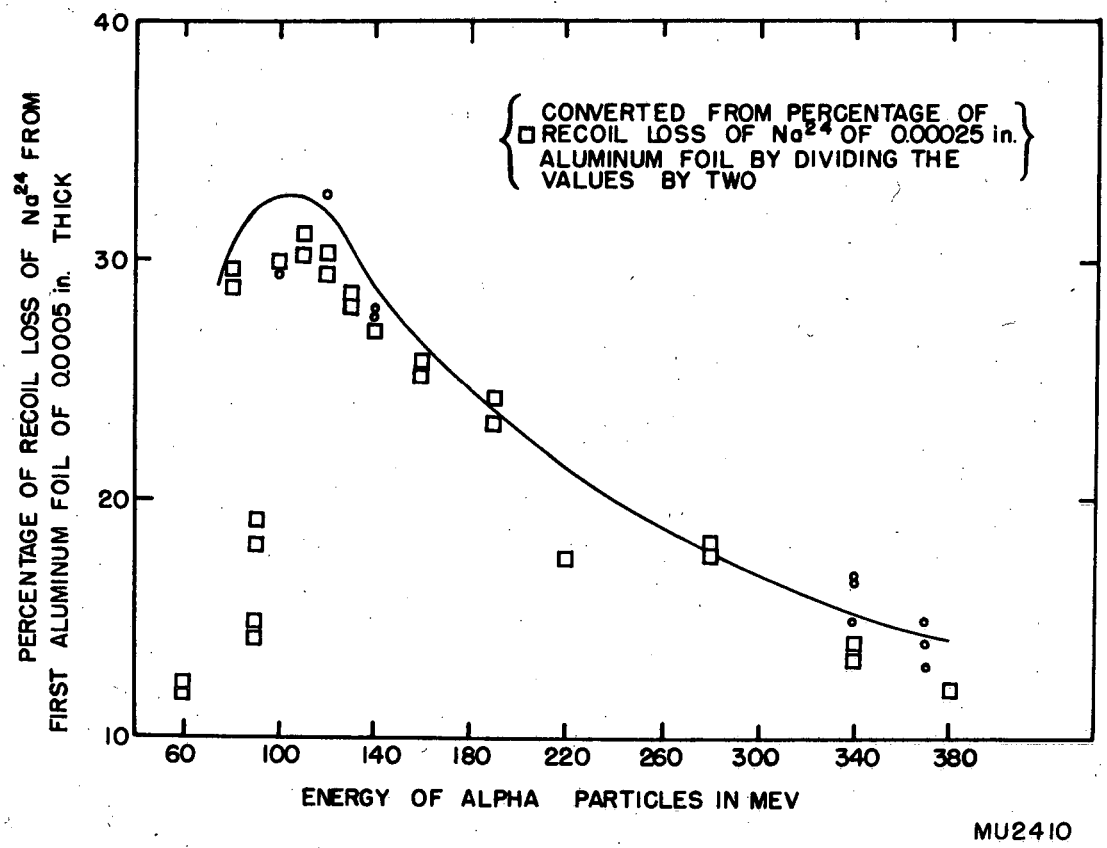

Figure 4

Part II

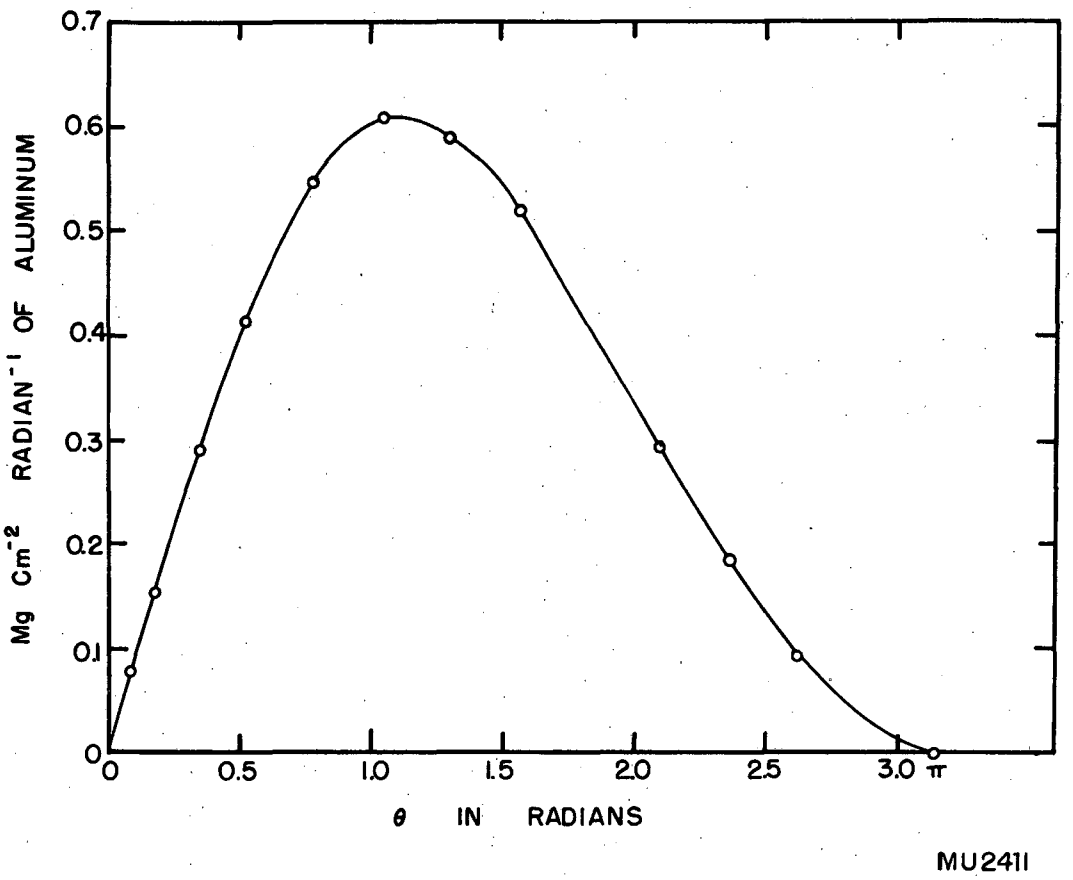

Figure 5

Part II

IX. REFERENCES

1. R. Serber, Phys. Rev. 72, 1114 (1947).

2. N. Bohr, Kgl. Danske Vid. Sels. Math.-fys. Medd. (Math.-phys. Comm., Acad. Sci. Copenhagen) 18, 8 (1940).

3. J. Knipp and E. Teller, Phys. Rev. 59, 659 (1941).

   J. H. M. Brunings, J. Knipp, and E. Teller, ibid., 60, 657 (1941).

4. M. S. Livingston and H. A. Bethe, Revs. Modern Phys. 9, 272 (1937).